Helmholtz and parabolic equation solutions to a benchmark problem in ocean acoustics

Elisabeth Larsson
Scientific Computing, Department of Information Technology, Uppsala University, Box 337, SE-751 05 Uppsala, Sweden

Leif Abrahamsson
Division of Systems Technology, Swedish Defence Research Agency, SE-172 90 Stockholm, Sweden

(Received 1 February 2002; accepted for publication 10 February 2003)

The Helmholtz equation (HE) describes wave propagation in applications such as acoustics and electromagnetics. For realistic problems, solving the HE is often too expensive. Instead, approximations like the parabolic wave equation (PE) are used. For low-frequency shallow-water environments, one persistent problem is to assess the accuracy of the PE model. In this work, a recently developed HE solver that can handle a smoothly varying bathymetry, variable material properties, and layered materials, is used for an investigation of the errors in PE solutions. In the HE solver, a preconditioned Krylov subspace method is applied to the discretized equations. The preconditioner combines domain decomposition and fast transform techniques. A benchmark problem with upslope–downslope propagation over a penetrable lossy seamount is solved. The numerical experiments show that, for the same bathymetry, a soft and slow bottom gives very similar HE and PE solutions, whereas the PE model is far from accurate for a hard and fast bottom. A first attempt to estimate the error is made by computing the relative deviation from the energy balance for the PE solution. This measure gives an indication of the magnitude of the error, but cannot be used as a strict error bound. © *2003 Acoustical Society of America.*
[DOI: 10.1121/1.1565071]

PACS numbers: 43.20.Mv, 43.30.Ma, 43.30.Gv [ADP]

I. INTRODUCTION

The parabolic wave equation (PE) is an important propagation model in underwater acoustics.[1,2] It is an approximation of the Helmholtz equation (HE) assuming one-way propagation within an angular sector. Its usefulness in solving propagation problems in ocean acoustics is well evidenced by the PE Workshops I and II.[3,4]

In this paper, we reexamine test case II from PE Workshop II, which is a low-frequency upslope–downslope propagation problem over a penetrable, lossy seamount. This test case, or a variant with an upslope wedge only, is frequently used to demonstrate the ability of PE modeling in range-dependent environments.[5,6] The success depends on two crucial factors: a slowly varying bathymetry, and moderate density and velocity contrasts at the water/bottom interface. Usually, the sound speed of the bottom is set to 1700 m/s for which the critical grazing angle is around 28°. In uphill propagation, wave angles steepen up, and when they become larger than the critical angle, energy starts to radiate into the bottom. For ''soft and slow'' bottoms with a small depth variation, most of the energy is transmitted into the bottom within the allowed angular domain of the PE model. This is the rationale of the common phrase ''the use of PE is justified if the range dependence is weak enough.'' However, in a real-world application it might be difficult to judge whether this condition is actually satisfied. Besides the bottom characteristics, the nature of the source is of considerable importance. It is easier to maintain the requirement of a small angular spread at high frequencies, by beamforming or filtering. Nevertheless, in ocean acoustics, PE is often applied to low-frequency shallow-water environments in which the applicability of PE modeling is less obvious. In this study, we extend the upslope–downslope problem to ''hard and fast'' bottoms. When the impedance of the bottom increases, transition zones of high angles of propagation and backscattering become more pronounced. At the same time, it leads to a gradual weakening of the validity of the assumptions behind PEs. It is worthwhile to find out what actually happens when a PE is pushed to, or beyond, the limit of its ability. The approach of the present study is mainly empirical in the sense that we compare numerical solutions of HE and PE. DeSanto[7] performed a theoretical study of the relation between HE and PE solutions. A theoretical analysis of the radiation conditions at modal cutoff in an upslope wedge is given by Pierce[8,9] and by Kath *et al.*[10] In the soft and slow bottom case, it was shown analytically that practically all the energy is transmitted into the bottom in a narrow beam at the cutoff point of the incoming mode. However, for hard and fast bottoms, part of the energy is backreflected in the water layer, and there is no beamforming of the energy shed into the bottom. This is confirmed by our numerical results, which also provide quantitative information on these phenomena for a benchmark problem.

We consider HE including appropriate boundary conditions as an exact model, although it is still an ideal description of a complicated reality. Thus, the solutions to HE provide a reference for the assessment of the quality of PE

 0001-4966/2003/113(5)/2446/9/$19.00

modeling. Since there are no closed-form analytic solutions to HE in range-dependent geometries, we have to rely on numerical solutions. If we could solve HE numerically for any given problem, we would do so. The reason for using approximations such as PE models is that solving HE is often too demanding from a computational point of view. For a realistic problem, the size of the spatial domain is typically a large number of wavelengths in both the range and depth directions. Even to obtain a crude geometrical resolution of the problem would require a fixed number of degrees of freedom per wavelength. Additional degrees of freedom are needed if near-field features are present. On the other hand, lossy media and leakage of energy out of the domain might lower the resolution requirements.

In general, discretization of the two-dimensional HE with, e.g., a finite-difference or finite-element method yields systems of equations whose size increases by at least the square of the frequency f. In fact, it has been shown that in order to keep the phase error below a given relative error tolerance, the number of grid points in the range direction must grow as $f^{1+(1/p)}$ for a pth-order accurate method.[11–15] This explains why systems of equations arising from the discretized HE cannot be solved by direct solution methods except for very small problems. The main difficulty is the large memory requirements, but the computational time is also an issue. Iterative methods often converge slowly for HE problems, since the coefficient matrix is ill-conditioned, especially for large problems. Standard preconditioning techniques do not perform well. However, the range of problems for which HE can be solved is steadily expanding due to the evolution of affordable computer power as well as algorithmic progress.

A prerequisite of the present work has been the development of a new preconditioned iterative HE solver. The resolution requirements discussed above show that a higher-order method is desirable in order to reduce problem sizes. The HE solver utilizes a fourth-order accurate finite-difference method. It means that the error is reduced by a factor of 16 when the step size is halved. This high rate of convergence is also of crucial importance for the following reason. To ascertain the accuracy of the numerical HE solution, we apply the method of self-validation. It implies that the solution is computed several times on successively finer grids until convergence is attained. Then, it is imperative that a satisfactory convergence criterion is met before the computer resources have been exhausted. For the current benchmark problem, this requirement cannot be achieved by a lower-order finite-difference or finite-element method.

As an alternative to HE solvers in ocean acoustics, the COUPLE code[16,17] has been used to generate reference solutions in terms of stepwise-coupled modes. The difficulty here is the slow rate of convergence for the staircase approximation of the computational domain. In layered media, this drawback can be overcome by orthogonal mappings of layers onto rectangles.[18] Occasionally, validation of COUPLE results has been done by intermodel comparisons.[19,20] In practice, the results have proven to be good enough for benchmark solutions as presented at PE Workshop II. However, as can be seen in more detail in Sec. IV, considerably higher resolution is needed for accurate solutions of upslope propagation problems over hard and fast bottoms.

It should be noted that we are addressing two very different validation problems in this paper. The first one is to ensure that the numerical solution of HE is accurate enough to serve as a reference. The second problem, which is the main topic, is the question of model validation of PEs. Besides comparisons of HE and PE solutions to a benchmark problem, we briefly indicate how to quantify the notion of ''weak range dependence'' and how to formulate computable criteria that ascertain the accuracy of the PE model.

An account of the codes and the numerics for the PE and HE solvers is given in Secs. II and III. It is a brief survey of previous papers. A more detailed description of the new parts of the preconditioning in the HE solver is given in the Appendix. The main results appear in Sec. IV. The focus is on the numerical experiments, and their implications for model validation of PEs, rather than physical or theoretical considerations.

II. THE PE SOLVER—JEPE

The development of JEPE (Jeltsch energy-conserving PE)[21,22] is the result of a team work at the Defense Research Establishment, Stockholm, Sweden. The code is continually updated to provide extended modeling capabilities and operational improvements. A number of new ideas have been tried and found useful.

A most significant feature of JEPE is the treatment of a range-dependent bathymetry. It is assumed that the physical parameters can be grouped into layers with the water layer at the top followed by one or several sediment or bedrock layers. The layer interfaces are assumed to vary smoothly by range, and the layer thickness must not shrink to zero. In JEPE, each layer is mapped onto a rectangle by an orthogonal, boundary-fitted transformation.[23] In this way, the special precautions needed in order to avoid an appreciable systematic error in the limit of an infinitesimal staircasing are avoided.[24] The PE model and the variation of media parameters are expressed in the new coordinates. The continuity conditions of pressure and velocity can then be treated as for the horizontally stratified case. The required normal derivative at the interface is merely approximated by a centered difference formula in the transversal coordinate direction.

The computational cost of any PE implementation is dominated by the step-by-step integration in range. The integrator in JEPE is a multistep, second derivative, fourth-order accurate method by Jeltsch.[25] The scheme is implemented by an automatic selection of an optimal step size so that a preset error criterion is fulfilled. Besides being cost effective, it relieves the user from specifying the range step.

Another cost-saving device in JEPE is to apply an adaptive choice of reference wave number in the formulation of the PE. When the propagation conditions change by range, or mode stripping occurs due to lossy media, the angular spread of energy varies. This in turn may prompt a new choice of reference wave number, which is computed according to Pierce.[26]

III. THE HELMHOLTZ SOLVER—FD4HE

The implementation of the HE solver denoted by FD4HE, where FD4 stands for fourth-order accurate finite differences, was developed at the Department of Scientific Computing, Uppsala University, Uppsala, Sweden. The code was originally designed for electromagnetic wave propagation in waveguides. Due to the similarities of two-dimensional transverse magnetic (TM) wave propagation in layered materials and acoustic wave propagation in fluid layers, it was rather straightforward to adapt the code to the current needs.

In the same way as in the JEPE code, an orthogonal transformation[23] of the layers of the physical domain onto rectangles is used. Rectangular domains are well suited for finite-difference discretizations, but there are still several possible choices. For interior grid points, we use a fourth-order Numerov scheme[15] that yields a compact nine-point stencil. The compactness facilitates the implementation of boundary conditions. Continuity conditions between layers are approximated by using one-sided fourth-order differences. At the vertical boundaries, we use nonreflecting boundary conditions of Dirichlet–to–Neumann type.[27] In these boundary conditions, modal expansions of the solution at the boundaries are used. The modes are computed by solving an eigenproblem,[28] and the discretization of that is done with a fourth-order accurate finite-element method.

The first difficulty lies in the fact that the system of equations that arises is very large. Direct solution methods, e.g., band Gaussian elimination, cannot be used because of their excessive memory requirements caused by fill-in. Instead, we use an iterative solution method, where the sparsity of the coefficient matrix is exploited. Since the matrix is complex and nonsymmetric, restarted GMRES[29] is a suitable choice. Then, a second difficulty emerges. The system of equations is also very ill-conditioned, and the iterative method does not converge without preconditioning. In an earlier paper,[28] Larsson suggested a preconditioning method that works well. The equations in the system were ordered in a domain decomposition fashion. A preconditioner based on sine transform matrices was constructed for the interior unknowns. Application of the preconditioner was then performed through the Schur complement method and fast Fourier transforms. It was found that the bottleneck of the computations was to form the Schur complement. In this work, that has been greatly improved by introducing a simpler approximation for the subproblems in the interior of the subdomains, which is used only when computing the Schur complement of the preconditioner. The simpler approximation involves a staircase approximation of the domain and a two-way adiabatic approximation in the range direction. The gain compared with the original preconditioning grows with problem size, and is about a factor of 3 with respect to the number of arithmetic operations for the test problems considered here, even though the iteration count increases. A more detailed description of the preconditioning is given in the Appendix.

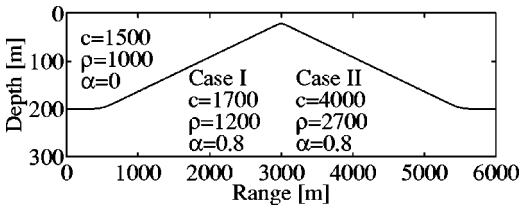

FIG. 1. Geometry of waveguide with plane symmetry and definition of media parameters, c is the speed of sound in m/s, ρ is the density in kg/m^3, and α is the absorption in dB/λ.

IV. BENCHMARK RESULTS

A. The benchmark problem

The test case is a two-layer waveguide with a symmetric bottom profile. A flat basin with a water depth of 200 m is followed by an upward-sloping bottom with an apex 22 m below the water surface. The slope of the bottom is 4°. In the experiments, we use different sound speeds and densities for the sediment layer. The extreme cases are the ''soft and slow'' and ''hard and fast'' bottoms denoted by case I and case II, respectively; see Fig. 1.

The bathymetry is slightly different from that of the second test case of PE Workshop II in two respects. First, the geometry is considered to be two-dimensional rather than three-dimensional with cylindrical symmetry. The reason is that we assume that the geometry continues with horizontal stratification outside the propagation range. This condition appears to be more realistic in cases with a significant amount of backreflection. It also facilitates the implementation of appropriate nonreflecting boundary conditions at the vertical boundaries of the computational domain. Another modification is the smoothing of corners of a polygonal bottom profile as suggested by Sundström.[30] It reduces scattering due to sharp changes in curvature, and facilitates the computation of a reference solution. For low frequencies, these alterations do not affect the main features of the original benchmark problem in any significant way. The source frequency is set to 25 Hz, and the source depth is 100 m. The source field is a modal sum of all three propagating modes at the initial range $x=0$. For computational purposes, the domain is truncated at depth $z=800$ m. Artificial absorption is introduced from $z=300$ m to $z=800$ m with a linear increase from 0.8 dB/λ to 10 dB/λ.

B. Self-validation of FD4HE

In an HE solution, the dominant error, and the error that must be suppressed by choosing a fine enough grid, is the phase error. Otto[15] has derived analytical expressions for the leading terms of the phase error for one propagating mode in a rectangular domain. Numerical experiments show that the phase error formulas give sharp predictions of the relative error. In a case with varying bathymetry, more than one propagating mode, and possibly mode coupling, it would be very difficult to analyze and derive an expression for the error. However, we can use the results for the rectangular domain as an approximate guide to a suitable mesh size. We specify a relative error tolerance τ, and then resolve according to the analytical criteria for a rectangular domain. We do

TABLE I. Self-validation of the HE solver. Given tolerances τ, and the maximum relative normwise difference between the finest solution and the coarser solutions.

	No. of points in z dir.	No. of points in x dir.	τ	max $\Delta_{\ell 0}$
Case I	479	2530	0.005	0
	403	2128	0.010	0.009
	339	1790	0.020	0.017
	305	1616	0.030	0.026
Case II	301	3008	0.0025	0
	255	2530	0.0050	0.017
	213	2128	0.0100	0.051
	179	1790	0.0200	0.088
	163	1616	0.0300	0.142

not expect to get an error bounded exactly by τ, but something of the same magnitude. For example, when more than one mode is propagating, even if the domain is rectangular, in the worst case each mode would contribute with a relative error τ.

For the convergence studies, a number of solutions on different grids have been computed for cases I and II, respectively. We will denote the computed solutions by $u_0,\ldots,u_n$, where u_0 is computed on the finest grid. For case I, $n=3$ and the problem sizes vary from about 400 000 to 1.2 million unknowns. For case II, we have used $n=4$ with problem sizes of approximately 200–900 thousand unknowns.

To get an idea of the sizes of the actual errors, we have computed relative normwise differences between the finest solution u_0 and the coarser solutions. The difference $\Delta_{\ell 0}$ for a vertical grid line was computed as

$$\Delta_{\ell 0}=\frac{\left(\int_0^{z_{\max}}\frac{1}{\rho(z)}|u_\ell-u_0|^2dz\right)^{1/2}}{\left(\int_0^{z_{\max}}\frac{1}{\rho(z)}|u_0|^2dz\right)^{1/2}}. \tag{1}$$

In Table I, a comparison between the given values of τ and the maximum values of the computed differences is shown. In Fig. 2, the differences are shown as a function of range. For a rectangular domain, a linear error growth in the direction of propagation is expected. For case I, we have linear growth, and by inspection of the differences, we conjecture that the errors are very close to τ at the outflow boundary. For case II, we get a large error growth halfway up the slope. This is probably connected with the excitation of higher modes that are not present in the source. Roughly estimated, the errors appears to be approximately of size 5τ at the outflow boundary. This reflects the more complicated behavior of the solution in case II.

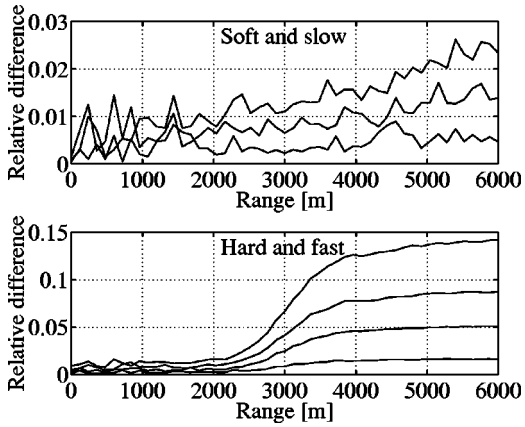

FIG. 2. Relative normwise differences between the finest and the coarser HE solutions. For case I (top) with given values of τ, from the uppermost curve and down, 0.03, 0.02, 0.01, and for case II (bottom) with $\tau=0.03$, 0.02, 0.01, 0.005.

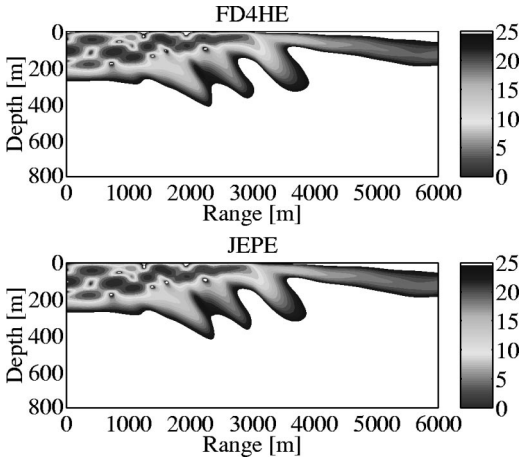

FIG. 3. Contours of the sound intensity in dB for the HE (top) and PE (bottom) solutions in case I.

A conclusion from these experiments is that the solution has converged enough to meet our requirements. Moreover, the errors on the finest grids are small compared with the differences between the HE and the PE solutions.

C. Comparison of HE and PE solutions

For the comparison of the HE and the PE solutions, we have used a wide-angle PE model due to Claerbout.[2] This model supports propagation angles below about 36°. We have compared the HE and PE solutions, both qualitatively and quantitatively. In Figs. 3 and 4, the sound intensity in dB is shown for the two solution methods applied to cases I and II. The picture for the soft and slow bottom case is well known. The source consists of three propagating modes.

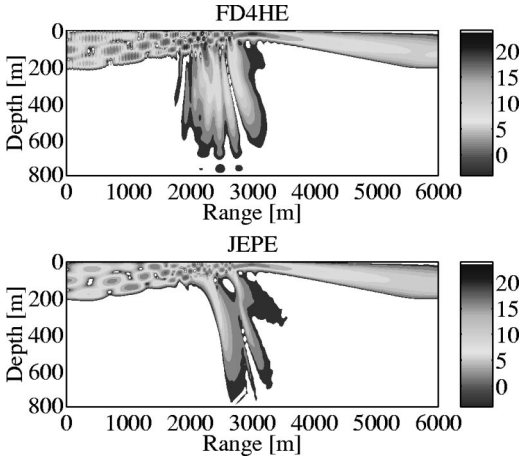

FIG. 4. Contours of the sound intensity in dB for the HE (top) and PE (bottom) solutions in case II.

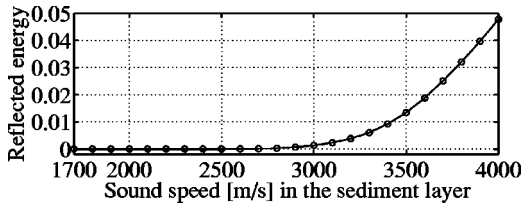

FIG. 5. Backreflected energy fraction measured at the left vertical boundary (the inflow boundary) as a function of bottom parameters. Both sound speed and density are increased linearly.

When they encounter their cutoff depths during uphill propagation, practically all the energy is transmitted into the bottom as narrow beams. The intensity contours in Fig. 3 are almost identical, whereas in the hard and fast case the solutions differ markedly. Transmission into the bottom at modal cutoff is still beam-like for the PE solution, whereas there is a wide angular spread of radiation for the HE solution. In addition, part of the energy is backreflected and still trapped in the water layer.

The relative amount of energy flux directed to the left is nearly 5%. This may seem like a rather small amount, but it is important to remember that the energy is proportional to the square of the amplitude, i.e., the total amplitude of the reflections is approximately 22%. Figure 5 shows how the backreflected energy increases by the characteristic impedance of the bottom. This picture was obtained by solving HE for a large number of cases in which ρ and c both were increased linearly from $\rho=1200$ and $c=1700$ to $\rho=2700$ and $c=4000$. The amount of backreflected energy was measured at $x=0$. It was calculated by using a modal expansion of the pressure field at $x=0$

$$u(x,z)=\sum_{m=1}^{3} A_m \exp(ik_m x)\psi_m(z) + \sum_{\mathrm{Re}\, k_m>0} B_m \exp(-ik_m x)\psi_m(z), \tag{2}$$

where the A_m coefficients are the known amplitudes in the source. Employing an approximate expression for the horizontal energy flux, yields the reflected energy fraction

$$E_r=\frac{\Sigma_{\mathrm{Re}\, k_m>0}\, \mathrm{Re}\, k_m |B_m|^2}{\Sigma_{m=1}^{3}\, \mathrm{Re}\, k_m |A_m|^2}. \tag{3}$$

In the limit case II, essentially only modes two and three are backreflected, and it was found that $|B_2|/|A_2|\approx 0.5$ and $|B_3|/|A_3|\approx 0.2$.

In Fig. 6, the normwise relative error for the PE solution, along a vertical grid line, is shown as a function of range. Here, we use the HE solution as our reference for the exact solution. The following expression was used for the error:

$$\Delta_{PE,HE}=\frac{\left(\int_0^{z_{\max}} \frac{1}{\rho(z)} |u_{PE}-u_{HE}|^2 dz\right)^{1/2}}{\left(\int_0^{z_{\max}} \frac{1}{\rho(z)} |u_{HE}|^2 dz\right)^{1/2}}. \tag{4}$$

In case I, the error has it largest value at the apex, after which it recovers. In case II, the error is 22% already at the inflow boundary. This is in accordance with the experiments above, where we predicted a total amplitude of 22% for the reflections. The HE and PE solutions use identical source functions. Therefore, the differences between the solutions at $x=0$ are solely due to reflections. Also in case II, the error recovers somewhat after the apex, but still cannot be deemed adequate.

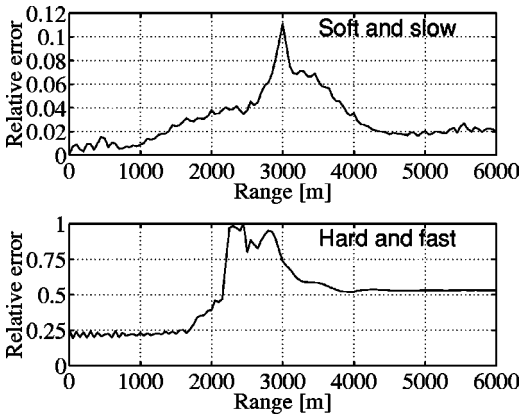

FIG. 6. Normwise relative difference between the PE and HE solutions, along a vertical grid line, as a function of range for case I (top) and case II (bottom).

Figure 7 shows how the error (4) evaluated at the apex $x=3000$ varies by the impedance of the bottom. In this picture, we have also included results for a very wide-angle PE model. As can be seen, there is a significant gain with the very wide-angle PE. However, also for this model the performance deteriorates as the bottom becomes more stiff. One reason is the excitation of modes with propagation angles larger than 60°, which is the limit often used for this model. Another reason is that there is a large amount of backreflection, which can never be approximated by a one-way model. Figures 8 and 9 show the amount of mode excitation for cases I and II over the entire range of propagation. In case I, only a small fraction of the energy propagates at large angles, and then only locally, close to the apex. The picture is different for case II. There, higher modes are excited along the upslope, and the energy in the higher modes is not at all negligible. The energy fractions were computed by doing local-mode expansions of the HE solution. An expression similar to Eq. (3) was used. However, here we relate modes with propagation angles θ_m larger than a given fixed angle to all of the modes, where

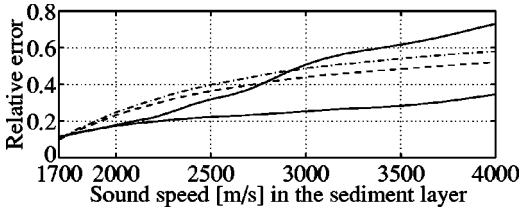

FIG. 7. Normwise relative difference between PE and HE solutions at the vertical grid line passing through the apex of the seamount. Density and sound speed in the sediment layers are varied linearly from case I to case II. The solid lines are the errors for a wide-angle PE (larger), and a very wide-angle PE (smaller). The relative deviation from the energy balance for the wide-angle (dashed line) and very wide-angle (dashed-dotted line) models are also shown.

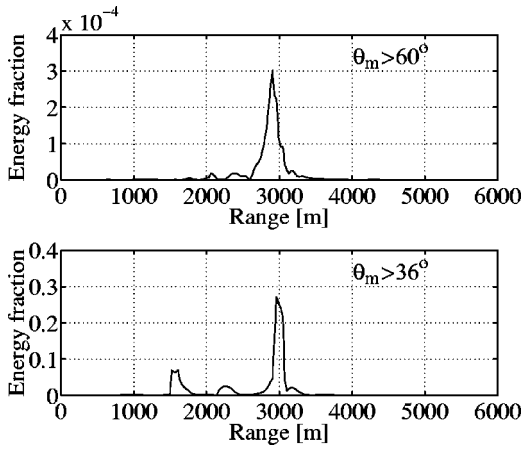

FIG. 8. Mode expansion of the HE solution for case I. The energy fractions for propagation angle θ_m larger than 36° and 60°, respectively. Note that the two scales are very different.

$$\cos\theta_m = \frac{\mathrm{Re}\, k_m}{k}, \tag{5}$$

and k is the wave number in the water layer.

In summary, the agreement between the HE and PE solutions is excellent in case I, whereas PE is incapable of handling case II. In case I, the incoming modes adapt adiabatically to the changing depth, and when the cutoff depth is encountered at an angle larger than the critical one, practically all the energy is emptied into the bottom. There is little mode interaction in this case. As the bottom becomes more stiff, there is a gradual increase of the critical grazing angle and the amount of mode excitation. At the same time, there is a weakening of the assumptions behind PE modeling. Theoretically, the situation can be improved somewhat by employing high-angle PEs, although it would be difficult to find out the ultimate borderline for any one-way model. One possibility is to invoke high-angle PEs in an adaptive way. A prerequisite for an automatic selection of an appropriate PE is a computational control device for the distribution of propagation angles within the field. We have done an experiment on self-control of the validity of PE solutions. The idea is to check the energy balance, which for the HE solution may be written

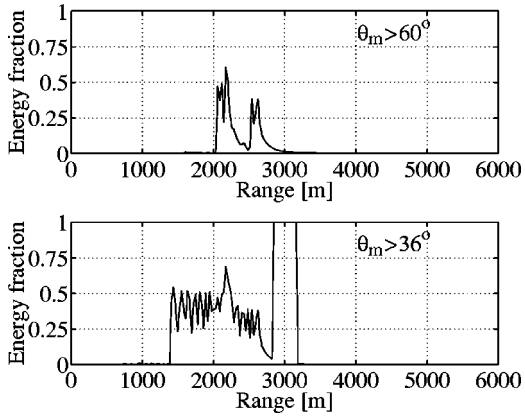

FIG. 9. Mode expansion of the HE solution for case II. The energy fractions for propagation angle θ_m larger than 36° and 60°, respectively.

$$F(0) = F(x) - \int_0^x \int_0^{z_{\max}} \mathrm{Im}\, k^2(z) |u(x',z)|^2 \; dz \; dx', \tag{6}$$

where

$$F(x) = \int_0^{z_{\max}} \mathrm{Im}\left(u \frac{\partial u}{\partial x} \right) \; dz \tag{7}$$

is proportional to the horizontal energy flux. The integral in Eq. (6) corresponds to the amount of absorbed energy due to attenuation over the range $(0,x)$. We try to construct an error indicator based on Eq. (6), which holds only approximately for PE solutions. Figure 7 shows the relative deviation from the energy balance (6) for the wide- and very wide-angle PE as a function of range. We see that the energy balance is far from being satisfied in case II. Apparently, this simple and inexpensive indicator works fairly well in this particular case. However, a comparison of the relative deviation from the energy balance and the error curves in Fig. 7 shows that the actual error is grossly overestimated for the very wide-angle PE in case II. Moreover, the estimator indicates a larger error in the very wide-angle model than in the wide-angle model, which is clearly in disagreement with the computed error results. Further work is needed to find more refined sensors.

V. SUMMARY

In conclusion, the results of the present work confirm the widely accepted belief that PE models are accurate for low-frequency propagation of acoustic waves over shallow oceans, provided that the depth variation and the density and velocity contrasts are moderate. High-angle PEs may extend the applicability to some degree. However, it is very difficult to predict when the conditions for their use are satisfied. Our calculations show that no PE model would do for hard and fast ocean bottoms with slight variations in bathymetry. The purpose of this paper has been to illuminate this issue quantitatively by accurate and comprehensive numerical solutions of the Helmholtz equation.

One difficulty of great practical concern is to develop computable criteria that measure the accuracy of the PE solution as it evolves in range. By an example, we have hinted at the possibility of introducing self-control. Evidently, indispensable tools for evaluation and further improvement of PE models are provided by the development of new, powerful HE solvers.

ACKNOWLEDGMENT

The first author would like to thank her advisor, Dr. Kurt Otto, for his constructive criticism.

APPENDIX: PRECONDITIONING OF THE ITERATIVE HELMHOLTZ SOLVER

A short description of the preconditioner constructed by Larsson[28] will be given here in order to point out the improvements implemented in this work.

First, the unknowns are separated into interface unknowns and interior unknowns. This domain decomposition type ordering yields a block system $Bu=g$ of the following form:

$$\begin{pmatrix} B_{00} & B_{01} \\ B_{10} & B_{11} \end{pmatrix} \begin{pmatrix} u_0 \\ u_1 \end{pmatrix} = \begin{pmatrix} g_0 \\ g_1 \end{pmatrix}. \tag{A1}$$

The largest block in the matrix is B_{11}, which corresponds to couplings between interior unknowns. It contains a number of subdomain problems, one for each layer in the physical domain. The subdomain problems are decoupled, except for the global nonreflecting boundary conditions at the vertical boundaries. Each subdomain problem is an HE problem with Dirichlet boundary conditions at the top and bottom boundaries. For these types of problems, effective preconditioning[14,15] techniques exist.

In a previous paper,[28] a preconditioner with the following structure was considered:

$$M = \begin{pmatrix} B_{00} & B_{01} \\ B_{10} & M_{11} \end{pmatrix}. \tag{A2}$$

The iterative method was then applied to $M^{-1}Bu=M^{-1}g$ in place of (A1). One of the steps in the preconditioning algorithm consists of solving a Schur complement system. That Schur complement of M is

$$\tilde{C} = B_{00} - B_{01}M_{11}^{-1}B_{10}. \tag{A3}$$

This is all very well, but building the Schur complement $\tilde{C}$ takes a lot of time. In this work, we have exchanged M_{11} in (A3) for an even simpler approximation in order to reduce the computational cost. The original M_{11} is a normal block approximation of the matrix B_{11}, utilizing sine transform matrices. The sine transform was chosen, because it corresponds to the analytical vertical eigenmodes of an HE problem with Dirichlet boundary conditions in a rectangular domain. This choice of M_{11} can be described as finding a least-squares approximation in a matrix sense to the original problem, but with constant coefficients for each vertical grid line within a subdomain. An important effect is also that the subdomain problems are completely decoupled.

A simpler approximation should achieve something similar, but with less arithmetic operations. In the previous work, we looked at the problem from a linear algebra point of view, and approximated the matrix. Here, we consider the continuous problem, and try to find an approximate formulation. Forming $\tilde{C}$ mainly consists of a large number of solves with M_{11} as the coefficient matrix, and the columns of B_{10} as right-hand sides. In a continuous setting, these right-hand sides correspond to source functions, and the solution vectors correspond to the solutions of a modified HE problem for those sources.

We begin by defining a modified continuous problem with properties similar to those of the discrete problem defined by M_{11}. We emphasize two properties. First, the subdomain problems must be independent of each other. Second, we want constant coefficients in the vertical direction. Then, we proceed with the source functions. The right-hand sides, i.e., the columns of B_{10}, have only a few nonzero elements. Each of those is treated as a point source in the continuous case. The strength of a source is obtained by a simple scaling of the corresponding element in B_{10}. Finally, we solve the continuous problems, and evaluate the solutions for pertinent grid points. The solution vectors obtained in this way are our approximation of $M_{11}^{-1}B_{10}$ in Eq. (A3).

The coefficients are made constant in the vertical direction by using, for each subdomain and each vertical grid line, the average value of all material properties, and requiring the bottom and interface curves to be of piecewise constant depth. All the subdomain problems are treated in the same way, and can be solved independently. We illustrate the solution process by studying one arbitrary subdomain and one right-hand side. For simplicity, we use a uniform partition of the range direction

$$h = \frac{x_{\max}}{N-1}, \quad x_j = (j-1)h, \quad j = 1,\ldots,N. \tag{A4}$$

The subdomain is divided into N slices of equal width h, but with individual constant depths d^j. Let the rectangular slice j have the vertical line $x=x_j$ as its centerline. Any parameter that is constant in the range direction within slice j is endowed with a superscript j. In slice j, there is a point source $s^j\delta(x-x_j)\delta(z-z_s)$, where s^j is the strength of the source, and (x_j, z_s) is the position. Note that s^j is zero in cells without sources, and if there are several sources in each cell, the different solutions can be superpositioned. In a rectangular domain, HE with constant coefficients is separable, i.e., we can write

$$u(x,z) = \sum_{m=1}^{\infty} \varphi_m(x)\psi_m^j(z), \qquad x_j - \frac{h}{2} \leqslant x < x_j + \frac{h}{2}, \quad j = 1,\ldots,N. \tag{A5}$$

The vertical eigenmodes are

$$\psi_m^j(z) = \sqrt{\frac{2}{d^j}} \sin\left(\frac{m\pi z}{d^j}\right). \tag{A6}$$

Insertion of the ansatz (A5) into the Helmholtz equation including the source terms yields

$$\sum_{m=1}^{\infty} (-\varphi_m''(x) - (k_m^j)^2\varphi_m(x))\psi_m^j(z) = s^j\delta(x-x_j)\delta(z-z_s), \qquad x_j - \frac{h}{2} \leqslant x < x_j + \frac{h}{2}, \quad j = 1,\ldots,N, \tag{A7}$$

where

$$k_m^j = \sqrt{k^2 - \left(\frac{m\pi}{d^j}\right)^2}, \tag{A8}$$

and k is the wave number in the current subdomain. We study a weak form of this equation, locally in slice j, by taking the scalar product with the modes ψ_n^j, which form an orthonormal basis. Then, we get

$$-\varphi_m''(x) - (k_m^j)^2\varphi_m(x) = s^j\delta(x-x_j)\psi_m^j(z_s). \tag{A9}$$

Equation (A9) tells us that the horizontal eigenfunctions should be continuous, and their derivatives should have jumps of size $-s^j\psi_m^j(z_s)$ at $x=x_j$. The solution for one mode is

$$\begin{aligned}
\varphi_m(x) &= A_m^j \exp(ik_m^j x) + B_m^j \exp(-ik_m^j x) \\
&\quad + s^j \psi_m^j(z_s) \frac{\sin(k_m^j(x-x_j))}{k_m^j}, \\
&\quad x_j - h/2 \leqslant x \leqslant x_j, \\
\varphi_m(x) &= A_m^j \exp(ik_m^j x) + B_m^j \exp(-ik_m^j x), \\
&\quad x_j < x < x_j + h/2.
\end{aligned} \tag{A10}$$

The solutions u for adjacent slices must be connected through suitable conditions of continuity. Here, we ignore couplings between different modes and the z dependence, and only enforce the continuity of the horizontal eigenfunction and its derivative between slices. Let $y_j = x_j + h/2 = x_{j+1} - h/2$ be the point where slices j and $j+1$ meet. For each mode, we get a system of equations for the unknown amplitudes A_m^j and B_m^j

$$\begin{aligned}
&A_m^j \exp(ik_m^j y_j) + B_m^j \exp(-ik_m^j y_j) \\
&\quad = A_m^{j+1} \exp(ik_m^{j+1} y_j) + B_m^{j+1} \exp(-ik_m^{j+1} y_j) \\
&\qquad + s^{j+1} \psi_m^{j+1}(z_s) \frac{\sin(k_m^{j+1}(y_j - x_{j+1}))}{k_m^{j+1}}, \\
&\qquad j = 1, \ldots, N-1, \\
&ik_m^j (A_m^j \exp(ik_m^j y_j) - B_m^j \exp(-ik_m^j y_j)) \\
&\quad = ik_m^{j+1} (A_m^{j+1} \exp(ik_m^{j+1} y_j) - B_m^{j+1} \exp(-ik_m^{j+1} y_j)) \\
&\qquad + s^{j+1} \psi_m^{j+1}(z_s) \cos(k_m^{j+1}(y_j - x_{j+1})), \\
&\qquad j = 1, \ldots, N-1.
\end{aligned} \tag{A11}$$

We also need two boundary conditions. We assume that no waves are entering the domain from the outside, and get

$$A_m^1 = 0, \quad B_m^N = 0. \tag{A12}$$

In practice, we cannot solve for all modes. Instead, we consider the number of modes that would be propagating if the attenuation was ignored. Mode m is propagating if k_m^j is real. The largest m for which the corresponding mode is propagating, at least in the deepest part of the subdomain, is given by

$$\max_j \left\lfloor \frac{\operatorname{Re} k d^j}{\pi} \right\rfloor. \tag{A13}$$

This gives us an idea of how many modes will contribute to the solution away from the vicinity of the source. We add a few extra modes for good measure, and never take less than ten. Let μ denote the number of modes that are selected for the solution. Solving the system (A11) for $m=1,\ldots,\mu$ gives us the amplitude coefficients. Consequently, the horizontal eigenfunctions are uniquely determined by Eq. (A10). For any point, the solution u can be approximated by truncating the sum in Eq. (A5) at $m=\mu$.

Overall, this method of solving the subdomain problems gives solutions very similar to the ones we want to approximate, i.e., those obtained by using the original subdomain preconditioner M_{11}. However, it seems to be difficult to capture the correct magnitude of the solution at the positions of the sources. The situation is not really improved by increasing the number of modes. It does not have to mean that the solutions are inaccurate. It could be that the matrix formulation has a slightly different effect, which is not modeled by our approximation. To cure that deficiency, an additional local solution technique is used. The equations for the unknowns in a few vertical grid lines around the source are extracted from M_{11} and B_{10}. The equations are then modified to implement homogeneous Dirichlet boundary conditions on all four boundaries. In most cases, the solutions of the local problems hardly bear any resemblance to the solutions of the subdomain problems. However, this method performs well regarding the magnitude of the solution close to the source. Although, for problems with real coefficients, some artificial damping is needed to avoid resonant solutions. The part of the local solution that is closest to the source is incorporated into our previously computed solution vector. Another difficulty is that solutions, where the sources are close to the vertical boundaries, are not good enough. This affects a few of the right-hand sides, and for those the original M_{11} matrix is used instead of the new approximation.

The great saving we make in using the new approximation is primarily that the systems of equations that are solved are of the order of the number of grid points in one spatial direction. These systems are narrow banded and relatively few, which also plays an important role. Finally, the subdomain solutions need only be evaluated in some grid points because of the sparsity of B_{01}; see Eq. (A3).

[1] F. D. Tappert, "The parabolic approximation method," in *Wave Propagation and Underwater Acoustics*, edited by J. B. Keller and J. S. Papadakis, Lecture Notes in Phys., Vol. 70 (Springer, Berlin, 1977), pp. 224–287.

[2] F. B. Jensen, W. A. Kuperman, M. B. Porter, and H. Schmidt, *Computational Ocean Acoustics* (AIP, New York, 1994).

[3] J. A. Davis, D. White, and R. C. Cavanagh, "NORDA Parabolic Equation Workshop," NORDA TN-143, Naval Ocean Research and Development Activity, Stennis Space Center, MS (1982).

[4] S. A. Chin-Bing, D. B. King, J. A. Davis, and R. B. Evans, *PE Workshop II: Proceedings of the Second Parabolic Equation Workshop* (Naval Research Laboratory, Washington, DC, 1993).

[5] F. B. Jensen and W. A. Kuperman, "Sound propagation in a wedge-shaped ocean with a penetrable bottom," J. Acoust. Soc. Am. **67**, 1564–1566 (1980).

[6] M. D. Collins, "Benchmark calculations for higher-order parabolic equations," J. Acoust. Soc. Am. **87**, 1535–1538 (1990).

[7] J. A. DeSanto, "Relation between the solutions of the Helmholtz and parabolic equations for sound propagation," J. Acoust. Soc. Am. **62**, 295–297 (1977).

[8] A. D. Pierce, "Guided mode disappearance during upslope propagation in variable-depth shallow water overlying a fluid bottom," J. Acoust. Soc. Am. **72**, 523–531 (1982).

[9] A. D. Pierce, "Augmented adiabatic mode theory for upslope propagation from a point source in variable-depth shallow water overlying a fluid bottom," J. Acoust. Soc. Am. **74**, 1837–1847 (1983).

[10] W. L. Kath, A. A. Minzoni, G. A. Kriegsmann, and E. L. Reiss, "Energy leakage and reflection in slowly varying waveguides," J. Acoust. Soc. Am. **93**, 182–187 (1993).

[11] A. Bayliss, C. I. Goldstein, and E. Turkel, "The numerical solution of the

Helmholtz equation for wave propagation problems in underwater acoustics,'' Comput. Math. Appl. **11**, 655–665 (1985).
[12] L. L. Thompson and P. M. Pinsky, ''Complex wave number Fourier analysis of the *p*-version finite element method,'' Comput. Mech. **13**, 255–275 (1994).
[13] F. Ihlenburg and I. Babuška, ''Finite element solution of the Helmholtz equation with high wave number. II. The *h*-*p* version of the FEM,'' SIAM (Soc. Ind. Appl. Math.) J. Numer. Anal. **34**, 315–358 (1997).
[14] K. Otto and E. Larsson, ''Iterative solution of the Helmholtz equation by a second-order method,'' SIAM J. Matrix Anal. Appl. **21**, 209–229 (1999).
[15] K. Otto, ''Iterative solution of the Helmholtz equation by a fourth-order method,'' Boll. Geof. Teor. Appl. **40**, 104–105 (1999).
[16] R. B. Evans, ''COUPLE: A User's Guide,'' NORDA TN-332, Naval Ocean Research and Development Activity, Stennis Space Center, MS (1986).
[17] F. B. Jensen and C. M. Ferla, ''Numerical solutions of range-dependent benchmark problems in ocean acoustics,'' J. Acoust. Soc. Am. **87**, 1499–1510 (1990).
[18] L. Abrahamsson and H.-O. Kreiss, ''Numerical solution of the coupled mode equations in duct acoustics,'' J. Comput. Phys. **111**, 1–14 (1994).
[19] R. A. Stephen, ''Solutions to range-dependent benchmark problems by the finite-difference method,'' J. Acoust. Soc. Am. **87**, 1527–1534 (1990).
[20] E. K. Westwood, ''Ray model solutions to the benchmark wedge problems,'' J. Acoust. Soc. Am. **87**, 1539–1545 (1990).
[21] L. Abrahamsson, L. Andersson, I. Karasalo, and A. Sundström, ''JEPE—a PE code for range-dependent fluid media,'' in *18th Scandinavian Symp. in Physical Acoustics* (Dept. of Physics, University of Bergen, Bergen, Norway, 1995), pp. 1–3.
[22] I. Karasalo and A. Sundström, ''JEPE—a high-order PE-model for range-dependent fluid media,'' in *Proc. 3rd European Conference on Underwater Acoustics* (Heraklion, Crete, Greece, 1996), pp. 189–194.
[23] L. Abrahamsson, ''Orthogonal grid generation for two-dimensional ducts,'' J. Comput. Appl. Math. **34**, 305–314 (1991).
[24] L. Abrahamsson and H.-O. Kreiss, ''Boundary conditions for the parabolic equation in a range-dependent duct,'' J. Acoust. Soc. Am. **87**, 2438–2441 (1990).
[25] R. Jeltsch, ''Multistep methods using higher derivatives and damping at infinity,'' Math. Comput. **31**, 124–138 (1977).
[26] A. D. Pierce, ''The natural reference wave number for parabolic approximations in ocean acoustics,'' Comput. Math. Appl. **11**, 831–841 (1985).
[27] J. B. Keller and D. Givoli, ''Exact non-reflecting boundary conditions,'' J. Comput. Phys. **82**, 172–192 (1989).
[28] E. Larsson, ''A domain decomposition method for the Helmholtz equation in a multilayer domain,'' SIAM J. Sci. Comput. (USA) **20**, 1713–1731 (1999).
[29] Y. Saad and M. H. Schultz, ''GMRES: A generalized minimal residual algorithm for solving nonsymmetric linear systems,'' SIAM (Soc. Ind. Appl. Math.) J. Sci. Stat. Comput. **7**, 856–869 (1986).
[30] A. Sundström, ''Ocean-acoustic test problems with a slowly varying bottom-slope: A missing class of benchmarks,'' in *Environmental Acoustics, Theoretical and Computational Acoustics*, edited by D. Lee and M. Schultz (World Scientific, Singapore, 1994), Vol. 2, pp. 835–848.